



The Thomas Jefferson National Accelerator Facility
Theory Group Preprint Series

JLAB-THY-00-01
FSU-SCRI-99-74

Additional copies are available from the authors.

The Southeastern Universities Research Association (SURA) operates the Thomas Jefferson National Accelerator Facility for the United States Department of Energy under contract DE-AC05-84ER40150.

The Overlap-Dirac Operator: Topology and Chiral Symmetry Breaking

Robert G. Edwards^(a), Urs M. Heller^(b), Rajamani Narayanan^(c)

(a) Jefferson Lab, 12000 Jefferson Avenue, Newport News, VA 23606, USA

(b) SCRI, Florida State University, Tallahassee, FL 32306-4190, USA

(c) American Physical Society, One Research Road, Ridge, NY 11961, USA

December 15, 1999

We review the spectral flow techniques for computing the index of the overlap Dirac operator including results relevant for SUSY Yang-Mills theories. We describe properties of the overlap Dirac operator, and methods to implement it numerically. We use the results from the spectral flow to illuminate the difficulties in numerical calculations involving domain wall and overlap fermions.

PACS. 11.15.Ha, 12.38.Gc. -

I. Overlap and domain wall Dirac operators

In these proceedings, we review some basic properties of the overlap Dirac operator and how its index can be computed by spectral flow techniques. One of the side results is that for fermions in the adjoint representation of $SU(N)$ we find evidence for fractional topological charge. The presentation is pedagogical with the intent of illustrating the origin of numerical difficulties in simulating overlap and domain wall fermions. Recent results from our work using overlap fermions can be found in references [1, 2, 3, 4].

The massive overlap Dirac operator derived from the overlap formalism [5] is

$$D_{ov}(\mu) = \frac{1}{2} [1 + \mu + (1 - \mu)\gamma_5 \epsilon(H_L(m))] \quad (1)$$

where $H_L(m)$ is a lattice hermitian Dirac-like operator describing a single fermion species with a large negative mass. The mass m is a regulator parameter for the theory. In this work, we use the hermitian Wilson-Dirac operator $H_w(m) = \gamma_5 D_{Wilson}(-m)$, although we have tested other fermion actions. The mass parameter $-1 < \mu < 1$ is related to the fermion mass by [6]

$$m_f = Z_m^{-1} \mu (1 + \mathcal{O}(a^2)). \quad (2)$$

The propagator for external fermions is given by

$$\hat{D}^{-1}(\mu) = (1 - \mu)^{-1} [D_{ov}^{-1}(\mu) - 1], \quad (3)$$

DISCLAIMER

This report was prepared as an account of work sponsored by the United States government. Neither the United States nor the United States Department of Energy, nor any of their employees, makes any warranty, expressed or implied, or assumes any legal liability or responsibility for the accuracy, completeness, or usefulness of any information, apparatus, product, or process disclosed, or represents that its use would not infringe privately owned rights. Reference herein to any specific commercial product, process, or service by trade name, mark, manufacturer, or otherwise, does not necessarily constitute or imply its endorsement, recommendation, or favoring by the United States government or any agency thereof. The views and opinions of authors expressed herein do not necessarily state or reflect those of the United States government or any agency thereof.

i.e. it has a contact term subtracted, which makes the massless propagator chiral: $\{\bar{D}^{-1}(0), \gamma_5\} = 0$.

A massless vector gauge theory can also be obtained from domain wall fermions [7], where an extra, fifth dimension, of infinite extent is introduced. In the version of ref. [8], one can show [9] that the physical (light) fermions contribute $\log \det D_{\text{DW}}$ to the effective action with the 4-d action

$$D_{\text{DW}} = \frac{1}{2} \left[1 + \mu + (1 - \mu) \gamma_5 \tanh \left(-\frac{L_s}{2} \log T \right) \right] \quad (4)$$

where T is the transfer matrix in the extra dimension and L_s its size. As long as $\log T \neq 0$ we obtain in the limit as $L_s \rightarrow \infty$

$$D_{\text{DW}} \rightarrow \frac{1}{2} [1 + \mu + (1 - \mu) \gamma_5 \epsilon(-\log T)]. \quad (5)$$

This is just the massive overlap Dirac operator up to the replacement $H_w \rightarrow -\log T$. It is easy to see that in the limit $a_s \rightarrow 0$, where a_s is the lattice spacing in the extra dimension (set to 1 above), one obtains $-\log T = H_w (1 + \mathcal{O}(a_s))$.

II. Some properties of the overlap Dirac operator

In many cases it is more convenient to use the hermitian version of the overlap Dirac operator (1):

$$H_o(\mu) = \gamma_5 D_{\text{ov}}(\mu) = \frac{1}{2} [(1 + \mu) \gamma_5 + (1 - \mu) \epsilon(H_w)]. \quad (6)$$

The massless version satisfies,

$$\{H_o(0), \gamma_5\} = 2H_o^2(0). \quad (7)$$

It follows that $[H_o^2(0), \gamma_5] = 0$, i.e. the eigenvectors of $H_o^2(0)$ can be chosen as chiral. Since

$$H_o^2(\mu) = (1 - \mu^2) H_o^2(0) + \mu^2 \quad (8)$$

this holds also for the massive case.

The only eigenvalues of $H_o(0)$ with chiral eigenvectors are 0 and ± 1 . Each eigenvalue $0 < \lambda^2 < 1$ of $H_o^2(0)$ is then doubly degenerate with opposite chirality eigenvectors. In this basis $H_o(\mu)$ and $D_{\text{ov}}(\mu)$ are block diagonal with 2×2 blocks, e.g.

$$D_{\text{ov}}(\mu) : \begin{pmatrix} (1 - \mu)\lambda^2 + \mu & (1 - \mu)\lambda\sqrt{1 - \lambda^2} \\ -(1 - \mu)\lambda\sqrt{1 - \lambda^2} & (1 - \mu)\lambda^2 + \mu \end{pmatrix}, \quad \gamma_5 = \begin{pmatrix} 1 & 0 \\ 0 & -1 \end{pmatrix}. \quad (9)$$

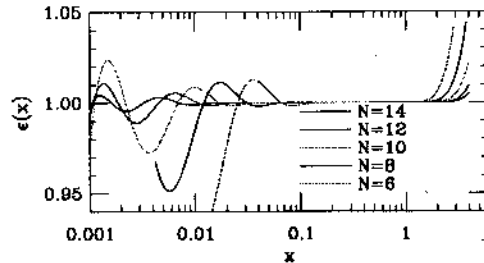


FIG. 1. Plots of the optimal rational function approximation to $\epsilon(x)$ for various order polynomials.

For a gauge field with topological charge $Q \neq 0$, there are, in addition, $|Q|$ exact zero modes with chirality $\text{sign}(Q)$, paired with eigenvectors of opposite chirality and eigenvalue 1. These are also eigenvectors of $H_o(\mu)$ and $D_{\text{ov}}(\mu)$:

$$D_{\text{ov}}(\mu)_{\text{zero sector}} : \begin{pmatrix} \mu & 0 \\ 0 & 1 \end{pmatrix} \quad \text{or} \quad \begin{pmatrix} 1 & 0 \\ 0 & \mu \end{pmatrix} \quad (10)$$

depending on the sign of Q .

We remark that from eigenvalues/vectors of $H_o^2(0)$ those of both $H_o(\mu)$ and $D_{\text{ov}}(\mu)$ are easily obtained. There is no need for a non-hermitian eigenvalue/vector solver! For example, the Ritz algorithm [10] will do just fine.

III. Implementations of the overlap Dirac operator

In practice, we only need the application of $D(\mu)$ on a vector, $D(\mu)\psi$, and therefore only the sign function applied to a vector, $\epsilon(H_w)\psi$. Since we need the sign function of an operator (a large sparse matrix) this is still a formidable task.

Methods proposed for this computation are:

- A Chebyshev approximation of $\epsilon(x) = \frac{x}{\sqrt{x^2}}$ over some interval $[\delta, 1]$ [11]. For small δ a large number of terms are needed.
- A fractional inverse method using Gegenbauer polynomials for $\frac{1}{\sqrt{x^2}}$ [12]. This has a poor convergence since these polynomials are not optimal in the Krylov space.

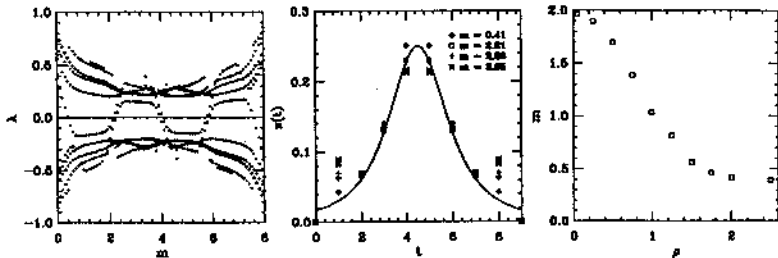


FIG. 2. Results for a single 8^4 instanton with radius $\rho = 2.0$ and Dirichlet boundary conditions. Left: spectral flow of $H_L(m)$, center: profile of the zero modes, right: mass crossing value as a function of the instanton radius.

- Use a Lanczos based method to compute $\frac{1}{\sqrt{x^2}}$ based on the sequence generated for the computation of $\frac{1}{x}$ [13].
- Use a rational polynomial approximation for $\epsilon(x)$ which can then be rewritten as a sum over poles:

$$\epsilon(x) \leftarrow x \frac{P(x^2)}{Q(x^2)} = x \left(c_0 + \sum_k \frac{c_k}{x^2 + b_k} \right) \quad (11)$$

The application of $\chi \leftarrow \epsilon(H_w)\psi$ can be done by the simultaneous solution of the shifted linear systems [14]

$$(H_w^2 + b_k)\phi_k = \psi, \quad \chi = H_w(c_0\psi + \sum_k c_k\phi_k). \quad (12)$$

One such approximation, based on the polar decomposition [15], was introduced in this context by Neuberger [16]. We use optimal rational polynomials [1]. The accuracy of this approximation is shown in Fig. 1.

We note that in all methods listed above, one can enforce the accuracy of the approximation of $\epsilon(x)$ for small x by projecting out the lowest few eigenvectors of H_w and adding their correct contribution exactly.

$$\epsilon(H_w) = \sum_{i=1}^n |\psi_i\rangle \epsilon(\lambda_i) \langle \psi_i| + P_1^{(n)} \text{App}[\epsilon(H_w)] P_1^{(n)}, \quad P_1^{(n)} = 1 - \sum_{i=1}^n |\psi_i\rangle \langle \psi_i|. \quad (13)$$

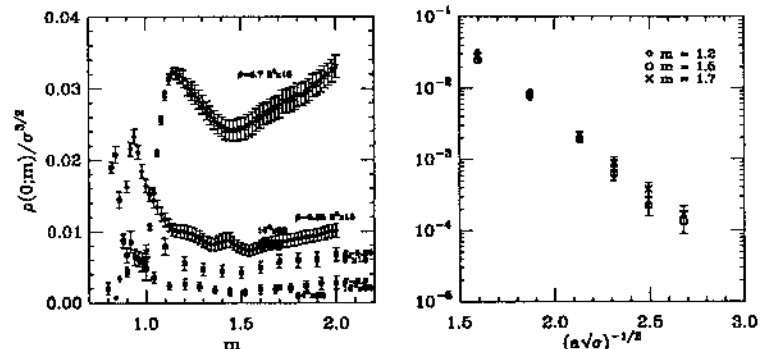


FIG. 3. On the left $\rho(0; m)$ of $H_w(m)$ for quenched Wilson $\beta = 5.7, 5.85$ and 6.0 . On the right, the approach of $\rho(0; m)$ to the continuum limit in the quenched theory at fixed masses.

To invert $D^4 D$ for overlap fermions, we have, generically, an outer CG method (a 4-d Krylov space search) and an independent inner search method for $\epsilon(H_w)\psi$ - maybe CG again. For domain wall fermions, on the other hand, a 5-d Krylov space search method is used. It may pay off to try to combine inner and outer CGs for overlap fermions by reformulating them into a 5-d problem [17, 18].

IV. Index defined via the Overlap formalism

The massless overlap Dirac operator is

$$D_{ow} = \frac{1}{2} [1 + \gamma_5 \epsilon(H_L)]; \quad H_L = \gamma_5 D_w(-m). \quad (14)$$

The index is given by $Q = \text{tr } \epsilon(H_L)/2$. We see Q simply counts the deficit of the number of positive energy states of H_L . A simple method of computing Q at some fixed m is via the spectral flow method [1]. Consider the eigenvalue problem

$$H_L(m)\phi_k(m) = \lambda_k(m)\phi_k(m), \quad \frac{d\lambda_k(m)}{dm} = -\phi_k^\dagger(m)\gamma_5\phi_k(m). \quad (15)$$

An efficient way to compute Q is to compute the lowest eigenvalues of $H_L(m)$ for $m > 0$. We can prove the number of positive and negative eigenvalues of $H_L(m)$ for $m < 0$ must be the same, so we slowly vary the mass m from $m = 0$ while keeping track of the levels

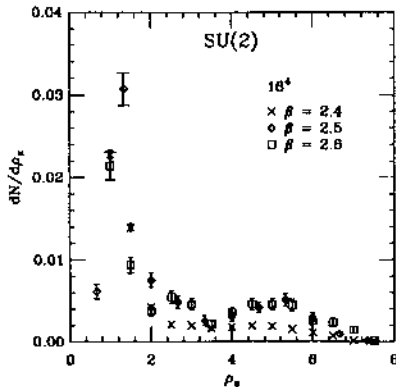


FIG. 4. Zero mode size distribution in lattice units for quenched 16^4 SU(2) Wilson gauge action.

crossing zero and direction of crossings up to some m . In this way, we get the topological charge as a function of m .

We note the mass m must be greater than the usual critical mass of $H_L(m)$, otherwise no topology change occurs and the overlap operator does not describe a massless chiral fermion. This critical mass value shifts from its free field value 0 to some positive value for non-zero gauge coupling. We should also choose a mass below 2 so that in the continuum limit there are no doubler contributions.

In Fig. 2, we show spectral flow results for a smooth background field of a single instanton [19]. There is a reflection symmetry about $m = 4$, namely the spectrum for $8 - m$ is opposite that of m . We see a mode crosses down in eigenvalue, then crosses up again near 2. There is a degeneracy of 3 for the modes just beyond 2. Hence, as we increase m we find a sequence of the index Q of 1, -3, 3, -1 and 0 for $m = 1, 3, 5$ and 8. The one-dimensional profile for the modes associated with the crossings are

$$z(t) = \sum_{\vec{n}} \phi_k^1(\vec{n}, t) \phi_k(\vec{n}, t) \quad (16)$$

which we compare with the continuum solution in the center panel of Fig. 2

$$z(t; c, \rho) = \frac{1}{[2\rho(1 + (\frac{t-c}{\rho})^2)^{3/2}]} \quad (17)$$

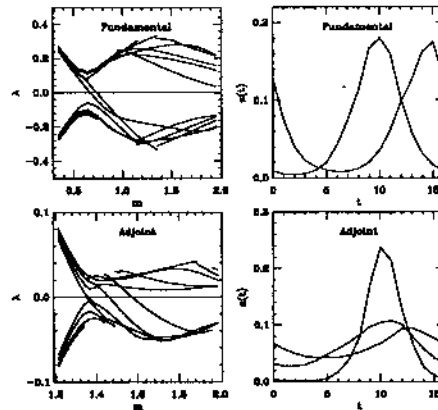


FIG. 5. Spectral flow and corresponding profile for SU(2) configurations with $I_a \neq 4I_f$ where I_a is the number of crossings in the adjoint rep. and I_f is the number of crossings in the fund. rep. There is a degeneracy of 2 in all crossings in the adjoint rep.

Also shown is the zero crossing point m as a function of ρ . We see that as the size of the instanton decreases the crossing point (the mass) increases.

As we turn on gauge fields, the picture of the flows complicates and we can find crossings throughout the mass region beyond the critical mass [21, 20]. Since we are interested in the zero modes at the crossings, we compute the density of zero eigenvalues $\rho(0; m)$ of $H_w(m)$ by fitting linearly to the integrated density

$$\int_0^\lambda \rho(\lambda') d\lambda' = \rho(0)\lambda + \frac{1}{2}\rho_1\lambda^2 + \dots \quad (18)$$

In Fig. 3 we show $\rho(0; m)$ for quenched SU(3) lattices. We see that for m beyond the critical mass region, the density $\rho(0; m)$ rises sharply to a peak, then drops but is never zero, hence the spectral gap is always closed. A similar result is also found for two flavor dynamical fermion backgrounds [21] (simulated with positive physical quark mass, *e.g.* not simulated in the super-critical mass region). From a size distribution, we observe the zero modes are on the order of one to two lattice spacings for m beyond the main band of crossings, namely for m in the “flat” region of $\rho(0; m)$. We find that a physical quantity, like the topological susceptibility, appears constant within errors in this “flat” region, indicating that these small modes make no physical contribution.

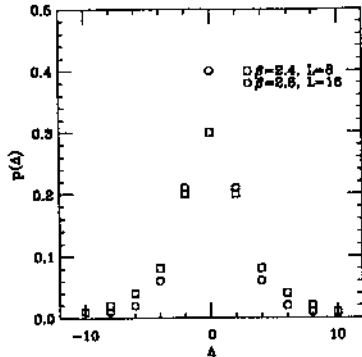


FIG. 6. Probability $p(\Delta)$ versus Δ for two gauge ensembles where $\Delta = I_a - 4I_f$.

For topology to change in a gauge field evolution, we must create dislocations. These produce the small modes observed above which force the spectral gap of $H_w(m)$ to be closed. In the right panel of Fig. 3 an empirical fit of the density to an exponential of the inverse lattice spacing is shown. This result implies the density is only zero in the continuum limit. The density of zero eigenvalues of $H_w(m)$, $\rho(0; m)$, is non-zero in the quenched case, but decreases rapidly with decreasing coupling [20]. Very roughly, we find $\rho(0; m)/\sigma^{3/2} \sim e^{-\beta\rho}$. We note the gauge action can be modified to reduce $\rho(0; m)$, or even eliminate it altogether at some fixed m [22].

In Fig. 4, we show the size distribution for quenched 16^4 SU(2) ensembles. The profile from Eq. (16) is used to define a size motivated by the t'Hooft zero mode in Eq. (17)

$$\rho_x = \frac{1}{2} \frac{\sum_t z(t)}{z_{\max}} \quad (19)$$

We see there is a large number of modes about 1 to 2 lattice units in size. There is a corresponding secondary peak around 5 lattice units and all the distributions are bounded in size. This result indicates that the size distribution of zero modes does not show evidence for a peak at a physical scale (as suggested by some models) even after we remove the small modes which are most likely lattice artifacts [20]. Instead, the observed scaling in lattice units is suggestive of a finite volume effect.

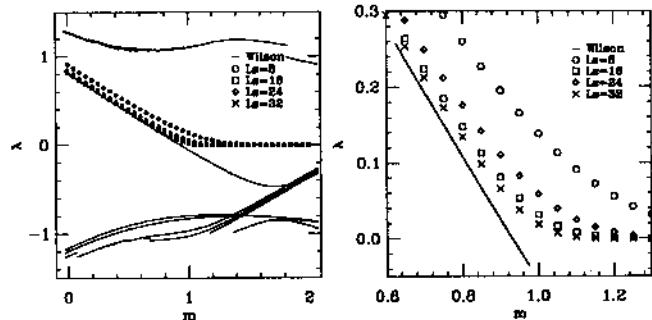


FIG. 7. Spectral flow of the hermitian domain wall Dirac operator $H_{DW}(m)$ and Wilson $H_w(m)$ on a single instanton background. Shown are 5D extents of $L_s = 8, 16, 24$ and 32 . For $L_s = 32$, only at a mass separation of 0.2 units from the crossing has the eigenvalue dropped to 10^{-3} .

V. Evidence for fractional topological charge

In a continuum background field with topological charge Q , the index of the massless Dirac operator in the *adjoint* representation is equal to $2NQ$ [24, 23]. Classical instantons carry integer topological charge and can thus only cause condensation of an operator with $2N$ Majorana fermions. Witten argued that a *bilinear* gluino condensate exists in SUSY YM. Self-dual twisted gauge field configurations, with fractional topological charge $1/N$ exist (t'Hooft), and could explain a bilinear gluino condensate. What about non-classical gauge field configurations?

The adjoint representation is real \Rightarrow spectrum of H_L is doubly degenerate: adjoint index can only be even. Are all even values realized, or only multiples of $2N$? To this end, we studied the flow in the adjoint representation on two SU(2) ensembles at the same fixed physical volume [23]. We do find configurations with $I_a = 4I_f$ (number of adjoint and fundamental crossings), but we also find configurations with $I_a \neq 4I_f$. An example is shown in Fig. 5.

To check if this evidence for fractional topological charge is a lattice artifact, we plot $\Delta = I_a - 4I_f$ in Fig. 6. Note that Δ takes on only even values. The probability of finding a certain value of Δ , $p(\Delta)$, is plotted for two ensembles in Fig. 6. We find that $p(\Delta)$ for $|\Delta| > 2$ decreases as one goes toward the continuum limit at a fixed physical volume. However, $p(\pm 2)$ does not decrease indicating that it might remain finite in the continuum limit.

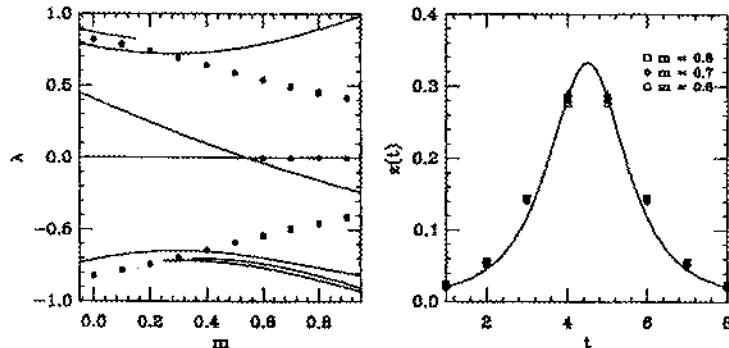


FIG. 8. Spectral flow of the overlap Dirac operator $H_o(m)$ and Wilson $H_w(m)$ on a single instanton background. On the right are the profiles of the overlap zero modes compared to the t'Hooft solution.

VI. Main problem for Overlap and Domain Wall fermions

The existence of small eigenvalues illustrated in Fig. 3 hampers the approximation accuracy and convergence properties of implementations of $\epsilon(H_w)$. Eigenvector projection both increases the accuracy of the approximation and decreases the condition number, e.g. of the inner CG.

The existence of small eigenvalues has implications also for domain wall fermions. One can show that the spectrum of $-\log T(m)$ of Eq. (4) around zero is the same as the spectrum of $H_w(m)$ [5]. While the small eigenvalues of $-\log T(m)$ don't appear to cause algorithmic problems for domain wall fermions, they can induce rather strong L_s dependence of physical quantities, and hence causing the need for large L_s .

VI-1. Domain Wall and Overlap-Dirac operator spectral flow for smooth SU(2)

As an illustration of the effects of low lying modes of $H_w(m)$, we show in Fig. 7 the spectral flow of the hermitian domain wall operator $H_{DW}(m) = \Gamma_3 D_{DW}(m)$ on a smooth $4^2 \times 8^2$ single instanton background with Dirichlet boundary conditions (BC). The Γ_3 includes a parity operator. Also shown is the corresponding hermitian Wilson $H_w(m)$ spectral flow. The “zero” DWF eigenvalue sets in slowly in L_s . We need $L_s \sim 1/\lambda_{\min}$ where λ_{\min} is the lowest eigenvalue of $H_w(m)$ (which is similar to the lowest eigenvalue

of $\log(T(m))$) for $\epsilon(-\log T(m)) \approx \tanh(-\frac{1}{2} \log T(m))$. In fact, the (almost) chiral zero mode eigenvalue $\lambda_{DW}(m) \sim \text{const} \times (1 - \tanh(\lambda_{\min}(m)L_s/2))$ for m beyond the crossing indicating a sensitivity to the hermitian Wilson operator eigenvalue.

In Fig. 8, we show a similar plot of the hermitian overlap Dirac operator $H_o(m)$ on a smooth 8^4 single instanton background with Dirichlet BC. There are strict zero modes after the crossing, $m = 0.6, 0.7$, and 0.8 . Also shown are the zero mode profiles for these masses which are quite similar and nicely follow the t'Hooft zero mode solution.

VII. Conclusions

The overlap Dirac operator has the same chiral symmetries as continuum fermions. It has exact zero modes in topologically non-trivial gauge fields. It is therefore well suited for a study of the interplay of topology, with its associated exact zero modes, and chiral symmetry breaking, determined by the density of small eigenvalues.

The creation of dislocations necessary for change of topology causes numerical difficulties with overlap and domain wall simulations. These dislocations are purely a property of the gauge actions used and are not a fundamental limitation of the chiral fermion formalisms. In practice, the projection technique used in the overlap simulations is vital to precisely control the adverse influence of the low lying zero modes of the hermitian Wilson operator. The same technique can be used for domain wall simulations, but it is more cumbersome. Further work is directed towards lowering (and possibly eliminating) the density of low lying zero modes. A dynamical HMC algorithm for the overlap Dirac operator has also been developed [4].

RGE would like to thank the organizers for a splendid workshop. The work of RGE and UMH has been supported in part by DOE contracts DE-FG05-85ER250000 and DE-FG95-96ER40979. RGE was also supported by DOE contract DE-AC05-84ER40150 under which SURA operates the Thomas Jefferson National Accelerator Facility.

References

- [1] R.G. Edwards, U.M. Heller and R. Narayanan, *Nucl. Phys. B*540 (1999) 457; *Parallel Computing* 25 (1999) 1395.
- [2] P.H. Damgaard, R.G. Edwards, U.M. Heller and R. Narayanan, hep-lat/9907016.
- [3] R.G. Edwards, U.M. Heller, J. Kiskis and R. Narayanan, hep-lat/9910041.
- [4] R.G. Edwards, U.M. Heller, J. Kiskis and R. Narayanan, Proceedings for NATO Advanced Research Workshop *Lattice Fermions and Structure of the Vacuum*, Dubna,

- Russia, Oct 1999; A. Bode, R.G. Edwards, U.M Heller, R. Narayanan, *ibid*.
- [5] R. Narayanan and H. Neuberger, *Nucl. Phys.* **B443** (1995) 305.
 - [6] R.G. Edwards, U.M. Heller and R. Narayanan, *Phys. Rev.* **D59** (1999) 094510.
 - [7] D.B. Kaplan, *Phys. Lett.* **B288** (1992) 342.
 - [8] Y. Shamir, *Nucl. Phys.* **B406** (1993) 90; V. Furman and Y. Shamir, *Nucl. Phys.* **B439** (1995) 54.
 - [9] H. Neuberger, *Phys. Rev.* **D57** (1998) 5417.
 - [10] B. Bunk, K. Jansen, M. Lüscher and H. Simma, DESY-Report (September 1994); T. Kalkreuter and H. Simma, *Comput. Phys. Commun.* **93** (1996) 33.
 - [11] P. Hernandez, K. Jansen, L. Lellouch, hep-lat/9907022.
 - [12] B. Bunk, *Nucl. Phys. Proc. Suppl.* **B63** (1998) 952.
 - [13] A. Borici, *Phys. Lett.* **B453** (1999) 46; hep-lat/9910045.
 - [14] A. Frommer, S. Güsken, T. Lippert, B. Nöckel, K. Schilling, *Int. J. Mod. Phys.* **C6** (1995) 627; B. Jegerlehner, hep-lat/9612014.
 - [15] N.J. Higham, Linear Algebra and Appl., Proceedings of ILAS Conference "Pure and Applied Linear Algebra: The New Generation," Pensacola, March 1993.
 - [16] H. Neuberger, *Phys. Rev. Lett.* **81** (1998) 4060.
 - [17] H. Neuberger, hep-lat/9909043.
 - [18] A. Borici, hep-lat/9909057.
 - [19] R.G. Edwards, U.M Heller, R. Narayanan, *Nucl. Phys.* **B522** (1998) 285.
 - [20] R.G. Edwards, U.M. Heller and R. Narayanan, *Phys. Rev.* **D60** (1999) 034502.
 - [21] R.G. Edwards, U.M Heller, R. Narayanan, *Nucl. Phys.* **B535** (1998) 403.
 - [22] P. Hernandez, K. Jansen, M. Lüscher, *Nucl. Phys.* **B552** (1998) 363.
 - [23] R.G. Edwards, U.M Heller, R. Narayanan, *Phys. Lett.* **B438**, 96, 1998.
 - [24] T. Eguchi, P.B. Gilkey and A.J. Hanson, *Phys. Rep.* **66** (1980) 213.